Rock physics and AVO applications in gas hydrate exploration

Yong Xu*, Satinder Chopra
Core Lab Reservoir Technologies Division,
301,400-3rd Ave SW, Calgary, AB, T2P 4H2
yxu@corelab.ca

ABSTRACT

Summary

Gas hydrates exhibit specific elastic properties, compared to other pore-filling fluids. Using AVO to understand the pore-filling fluids, this paper investigates the AVO characteristic in gas hydrate-filling rocks and explores the potential of AVO applications in the gas hydrate exploration.

Introduction

The energy tied in gas hydrates is believed to exceed the worldwide hydrocarbon deposits. So, gas hydrates are increasingly being recognized as a potential future energy source. In addition to this, accurately mapping the hydrate locations and contents prevents drilling hazards in oil and gas production in hydrate rich areas. Gas hydrates are ice-like crystalline solids composed of water molecules surrounding gas molecules. The presence of hydrates was first recognized through the characteristic BSRs (bottom simulating reflectors) on conventional seismic sections. BSRs are generated by the impedance contrasts between the hydrated sediments above and the free-gas or brine-saturated sediments below. Seismic data from Mackenzie Delta, Canada clearly show BSRs, which cross the background geological structures (see *Fig. 1*). Besides BSRs, it is important to identify gas hydrate deposits and estimate the content of hydrates. A key to obtain this from seismic data is rock physics – a link between seismic velocity/attenuation and internal rock structure. Elastic properties of hydrates have been studied by many researchers (Collett, Lee, Spence, Guerin, etc.). Some valuable relationships between the elastic properties and hydrate content have been derived. In the context of oil and gas exploration, AVO has been successfully used as a direct indicator of pore fluids on seismic data. Studies on AVO methodology applied to hydrate deposits were conducted by Ecker et al (1998). In their studies, some assumptions on the hydrate velocity models were made with the lack of in-situ elastic properties of hydrates. A recent well drilled through the hydrate zone with full suite of logs from Mackenzie Delta was used in this paper. AVO will be investigated in terms of fluid contacts, hydrate contents, and possibility to estimate the hydrate content from seismic data.

Well log data

Well logs at Mallik 2L-38 gas hydrate research well were acquired by Schlumberger Ltd in 1998. The well was drilled to investigate gas hydrates in a

collaborative research project among Japan National Oil Company, Japan Petroleum Exploration Company, Geological Survey of Canada, and the U.S. Geological Survey. It is located in the Mallik area in Mackenzie Delta, NWT, Canada. *Fig. 2* shows the key portion of well logs with high gas hydrate content. A large column of the shallow portion of the well at the shallow is permafrost zone, with high velocity. The gas hydrates in well 2L-38 locate at the transition between Mackenzie Bay and Kugmallit sequences. From the gamma ray log and hydrate content curves, it is noticed that most of the hydrates fill the pores of the sandy rocks.

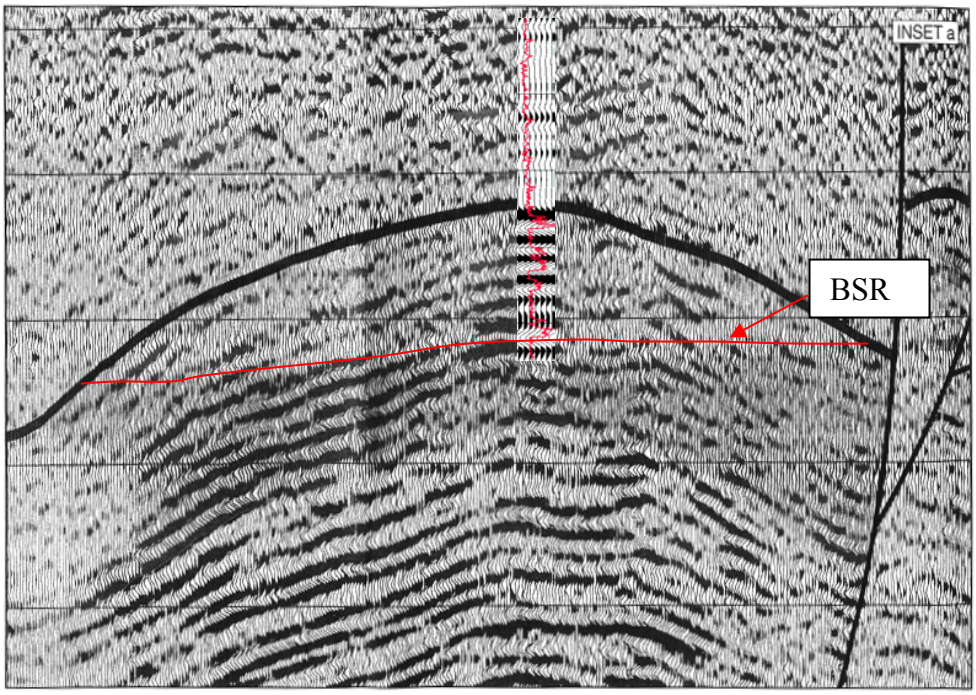

Fig. 1: Seismic section from Mackenzie Delta shows BSR and tie with synthetic from well 2L-38 (Geological Survey of Canada Bulletin, 544).

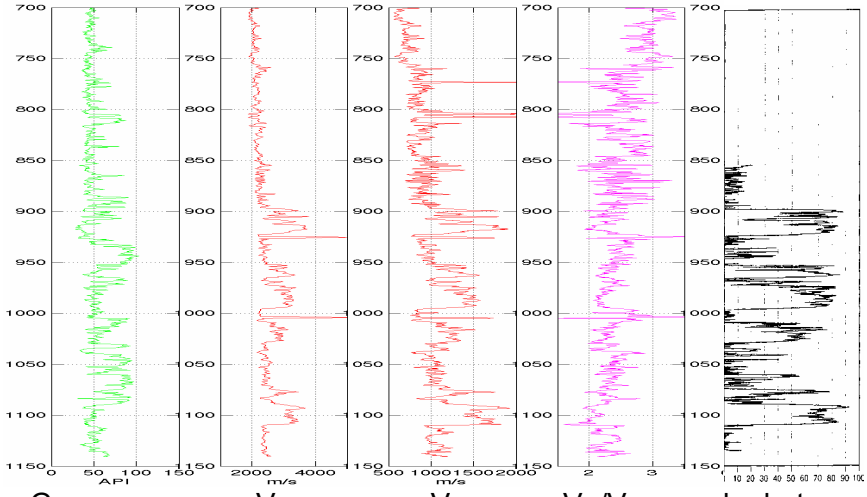

Fig. 2. Log curves from well 2L-38: Gamma ray, P velocity, S velocity, Vp/Vs ratio, and hydrate contents.

Rock physics and petrophysics

Fig. 3 (a) shows the cross-plot of P wave and S wave velocities from 2L-38 well logs. On these cross-plots, the clastic mud-rock lines after Castagna, which are the empirical linear relationships between Vp and Vs, are overlaid on the well logs. The well logs without hydrate content fit these Castagna's mud-rock lines generally. It can be seen the gas hydrate samples fall below the shale mud-rock line. The Vp and Vs for hydrate bearing rocks are following an approximated linear trend. Lee and Collett (2001) obtained the linear relationship as Vp = 1.452Vs+1031 m/s. There is 1.5m thick free-gas just below the major hydrate zone. On the cross-plots, the free gas zone shows a good separation from other fluid filling rocks and fits the typical gas sand.

Hydrate shows a large separation from other wet sand and shale on the cross-plot of Vp and Vs. The cross-plot shows Vp/Vs for hydrate is higher than sand or shale with similar P wave velocity. Both P wave and S wave velocities of hydrate are affected by hydrate concentration. Lee et al. (2002) gave the relationship between P wave velocity and S wave velocity and hydrate concentration. In other word, the hydrate concentration can be indicated from the P wave or S wave velocities.

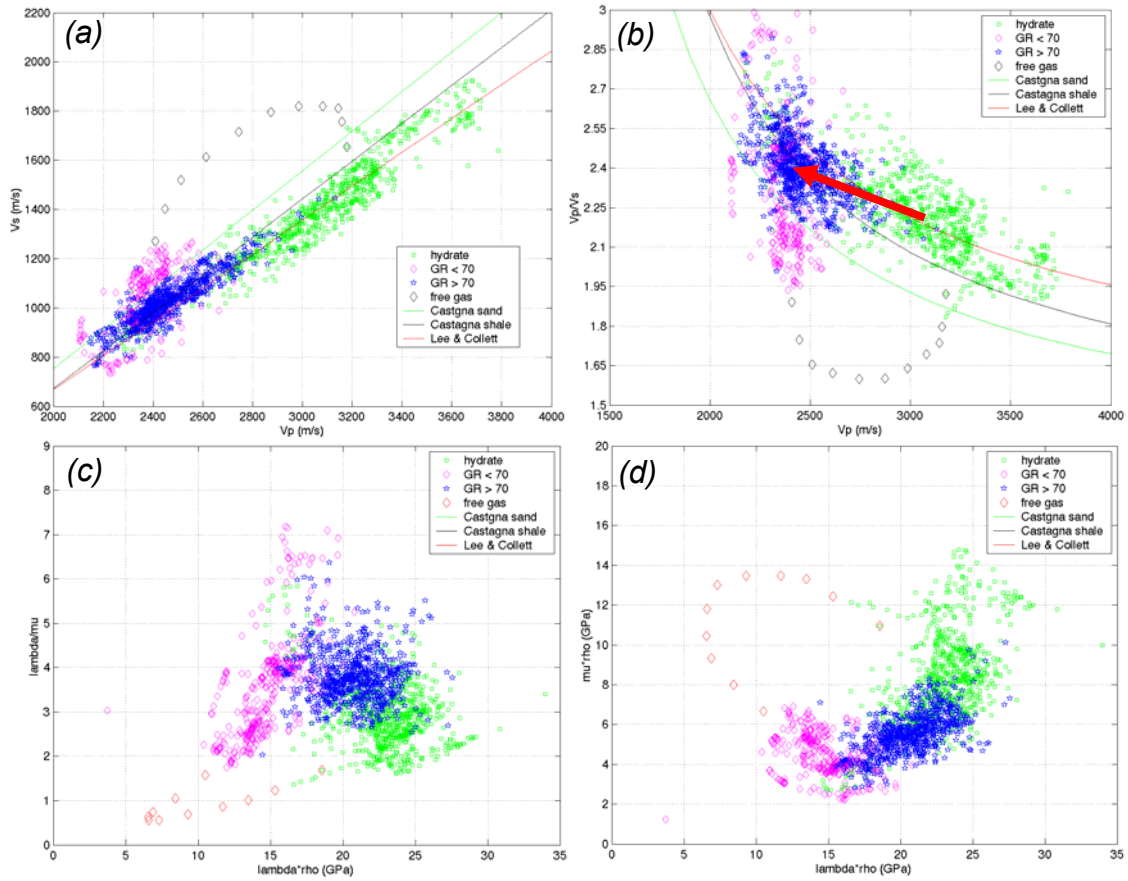

*Fig. 3, cross plot of elastic parameters from well logs of well 2L-38: (a) Vp vs. Vs; (b) Vp vs. Vp/Vs; (c) lambda*rho vs. lambda/mu; (d) lambda*rho vs. mu*rho.*

In Figure 3, the cross-plots of Lame's parameters are also shown. Usually the incompressibility is sensitive to gas saturation in clastic reservoir. From the cross plots in Figure 3, P velocity and S velocity are more sensitive to hydrate concentration than other parameters.

AVO responses and seismic methods

The existence of hydrate can be indicated from the increase in P wave velocity. But P wave velocity cannot be used to uniquely discriminate between hydrate deposition and other lithology contrast. S wave velocity becomes important. Seismic amplitude variation with offset analysis may be used for this purpose. Ecker at al. observed amplitude increase with offset on a BSR. A few factors affect the AVO responses at the BSR: the hydrate contact mode within the pore space, the hydrate concentration, and the fluid type and thickness below hydrate.

Free gas usually exists beneath the hydrate. Hydrate seals the free gas. Ecker et al. (2001) described a large free gas zone under hydrate using seismic velocity. Increase in P-velocity in hydrate and decrease in free gas give a large contrast and significant AVO response.

In *Fig. 4*, the reflection coefficients at a single interface between hydrate and other lithology and pore fluid are calculated. BSR with hydrate over free gas shows a strong increasing AVO response. The hydrate over wet sand or shale shown a strong zero offset reflection and dimming AVO.

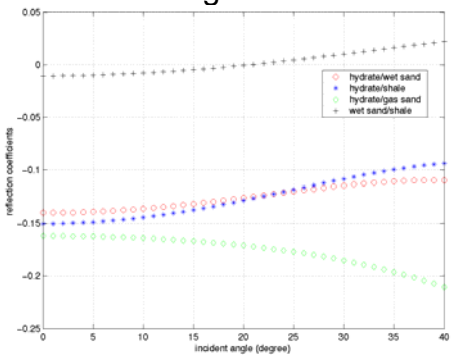

Figure 4. Single interface AVO response between hydrate and other lithology and pore fluids.

Free gas existence under hydrate in 2L-38 is verified by the log analysis (GSC Bulletin 544). The free gas zone is about 1.5 meter thick. AVO modeling with commonly used wavelength in the seismic cannot create obvious AVO effect due to such a thin zone (*Fig. 5 (a)*). When the gas zone is thickened, the bright AVO response between the hydrate and free gas shows up (*Fig. 5 (b*)).

In 2L-38, high hydrate concentration zones interbed low concentration zone. There are a few hydrate accumulation cycles: hydrate concentration increases gradually as depth increases, and drops to very low level and start the next cycle

of accumulation. This is indicated on *Fig. 5*. Generally, the hydrate exists in clean sands. The large high to low concentration drop also happens inside the sand body. With the thickened free gas sand, the AVO at BSR is a strong trough at zeros offset and increase with offset. Inside the hydrate zone, the accumulation cycle boundaries create strong reflection at zero offset and a dimming AVO.

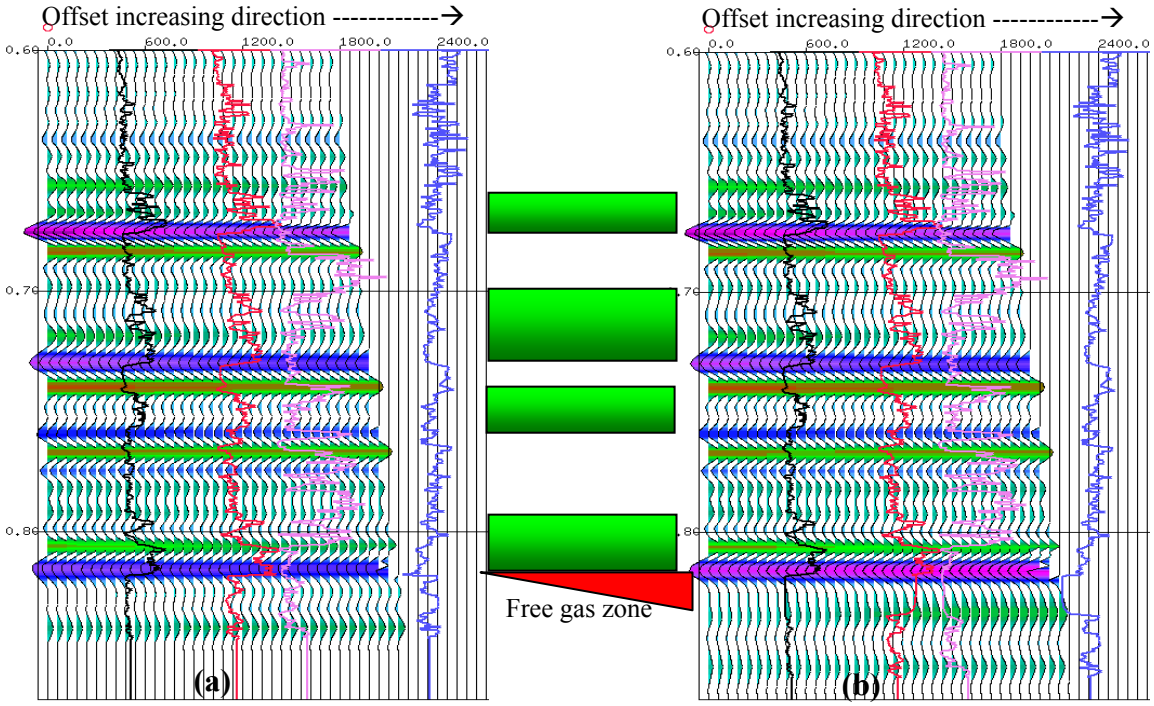

Figure 5, AVO response from original well logs and thickened bottom free gas: (a) the original well log with 1.5 m free gas; (b) the 20 m free gas. The gas bars indicate high hydrate concentration zones. Black curve is Vp log; the red is Vs; the purple is gamma ray; the blue is Vp/Vs.

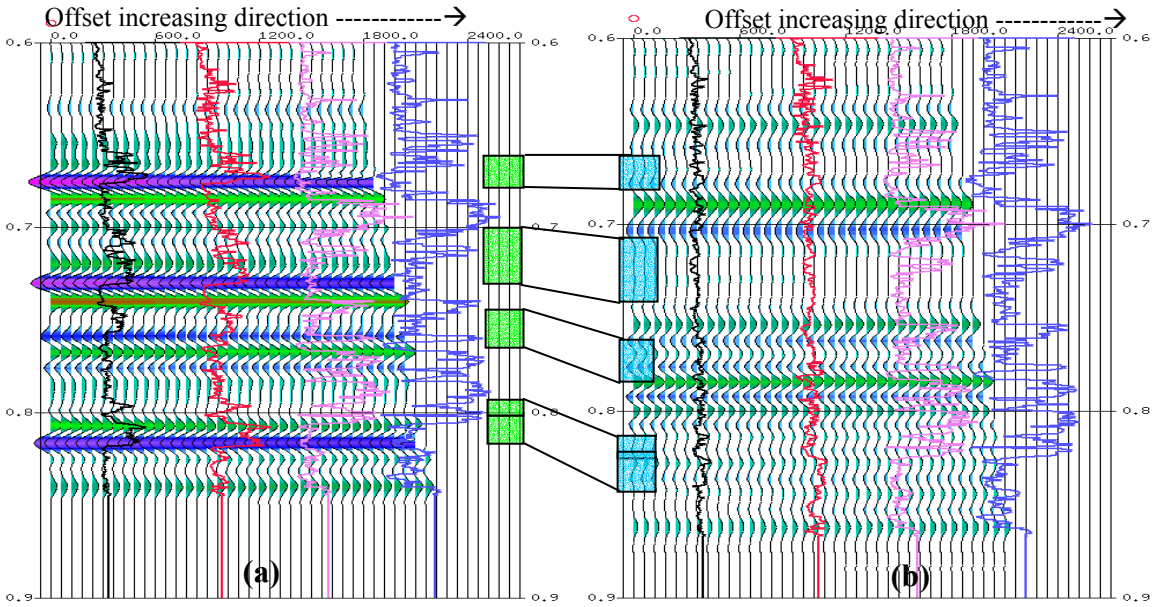

Figure 6. AVO gathers of (a) original hydrate concentration of 2L-38 and (b) zero hydrate concentration from fluid substitution: the color filled bars indicated the original high hydrate concentration zone (in green) and after brine substitution (in cyan). Black curve is Vp log; the red is Vs; the purple is gamma ray; the blue is density.

Based on Biot-Gassmann theory and hydrate contact mechanism (Lee, 2002), the hydrate is substituted by brine. The AVO gathers for hydrate and brine filling are shown in *Fig. 6*. Two gathers are plotted using the same amplitude color-coding. The brine saturated gather shows much lower amplitude than the hydrate filled gather. Based on AVO gathers in *Fig. 6*, the P and S velocity contrasts are extracted. The fluid factors, the difference between P velocity reflectivity and reduced S velocity reflectivity, are calculated. The scalar to reduce S velocity reflectivity is calculated from Castagna's clastic mud-rock line. On the fluid factors, the large hydrate concentration contrasts show a strong trough.

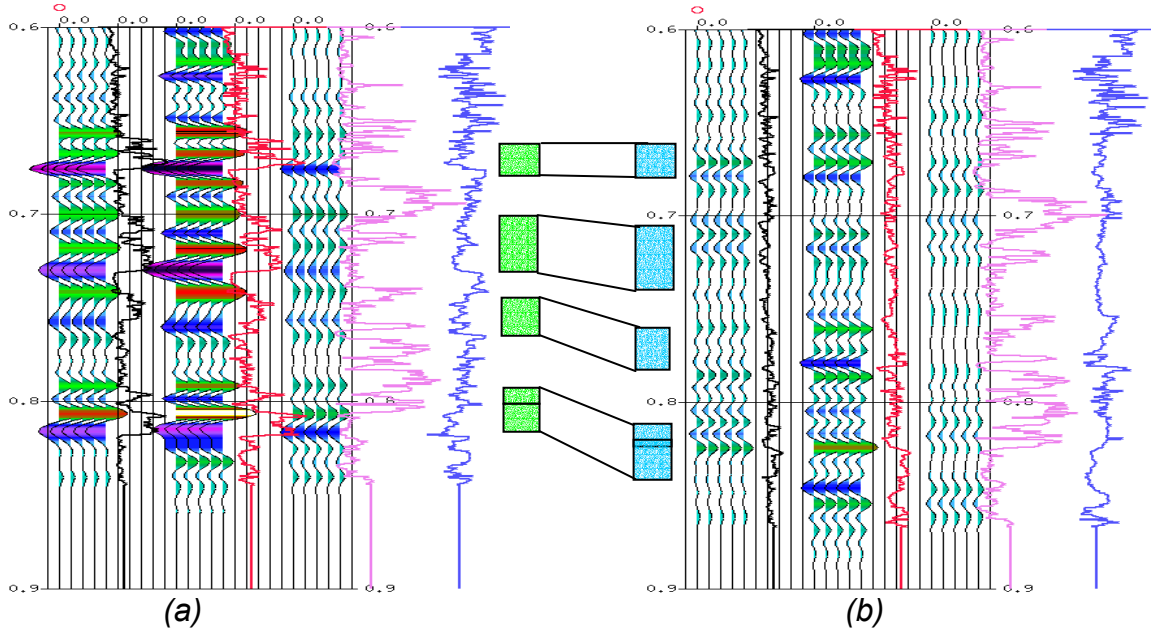

Figure 7. AVO attributes extracted from AVO gathers in Figure 6: (a) original hydrate concentration; (b) brine substitution. P and S velocity reflectivity and fluid factor are displayed in each panel. The color filled bars indicated the original hydrate zones. Black curve is Vp log; the red is Vs; the purple is gamma ray; the blue is Vp/Vs.

A 2D model is generated to model the hydrate concentration lateral variations. The velocities and density of the 2D model are shown in *Fig. 8*. The P and S velocity show a significant variation as hydrate concentration changes from the original of 2L-38 to zero. A 2D pre-stack dataset is modeled using the velocities and density grids and Zoepprtiz equations. P and S reflectivity are extracted from this dataset and fluid factor section is calculated using the P and S reflectivity. The fluid factor section shows a hydrate concentration mapping.

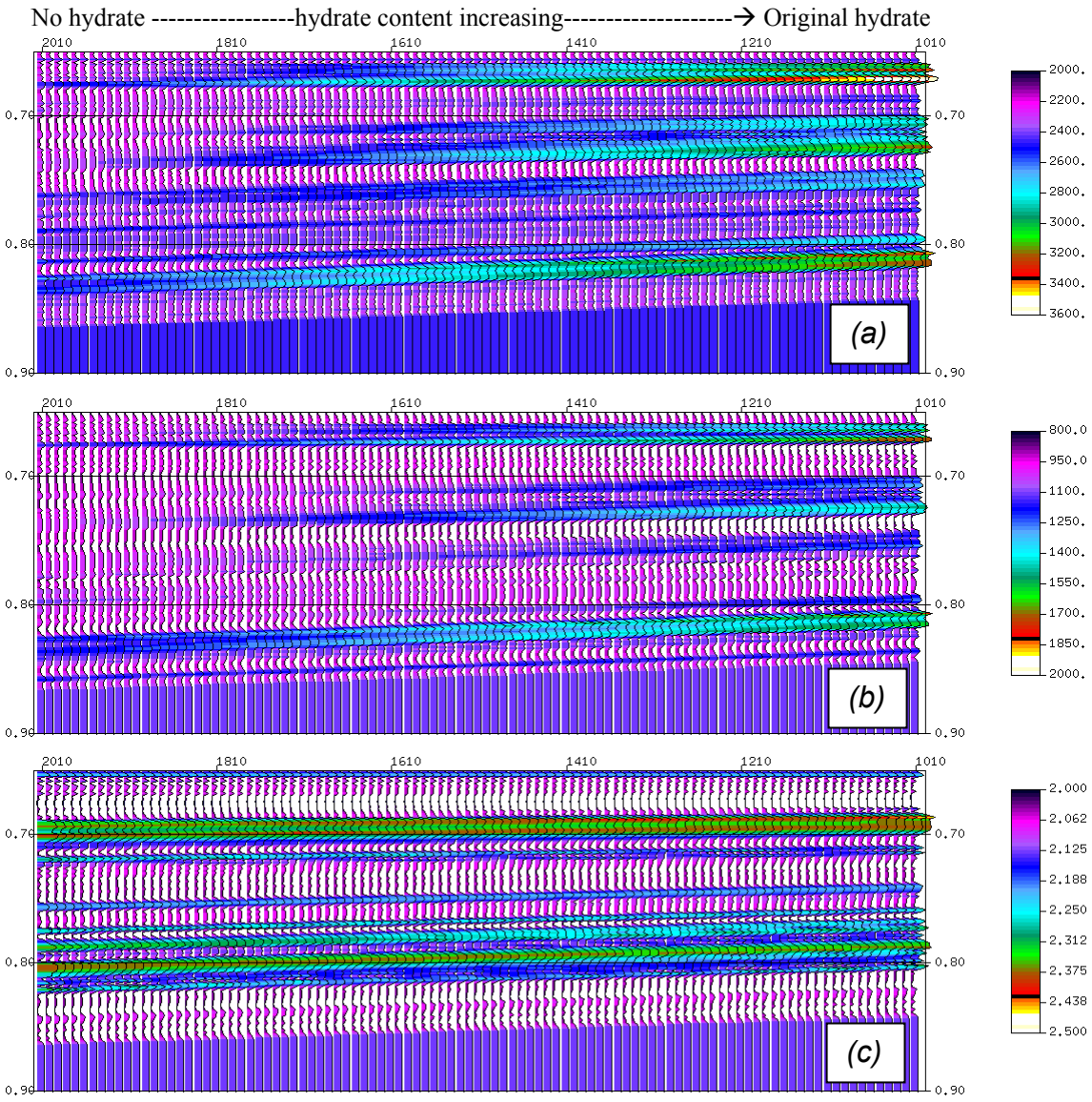

Fig. 8: P and S velocity and density of 2D model using original 2L-38 logs and fluid substitutions: (a) P velocity; (b) S velocity; (c) density.

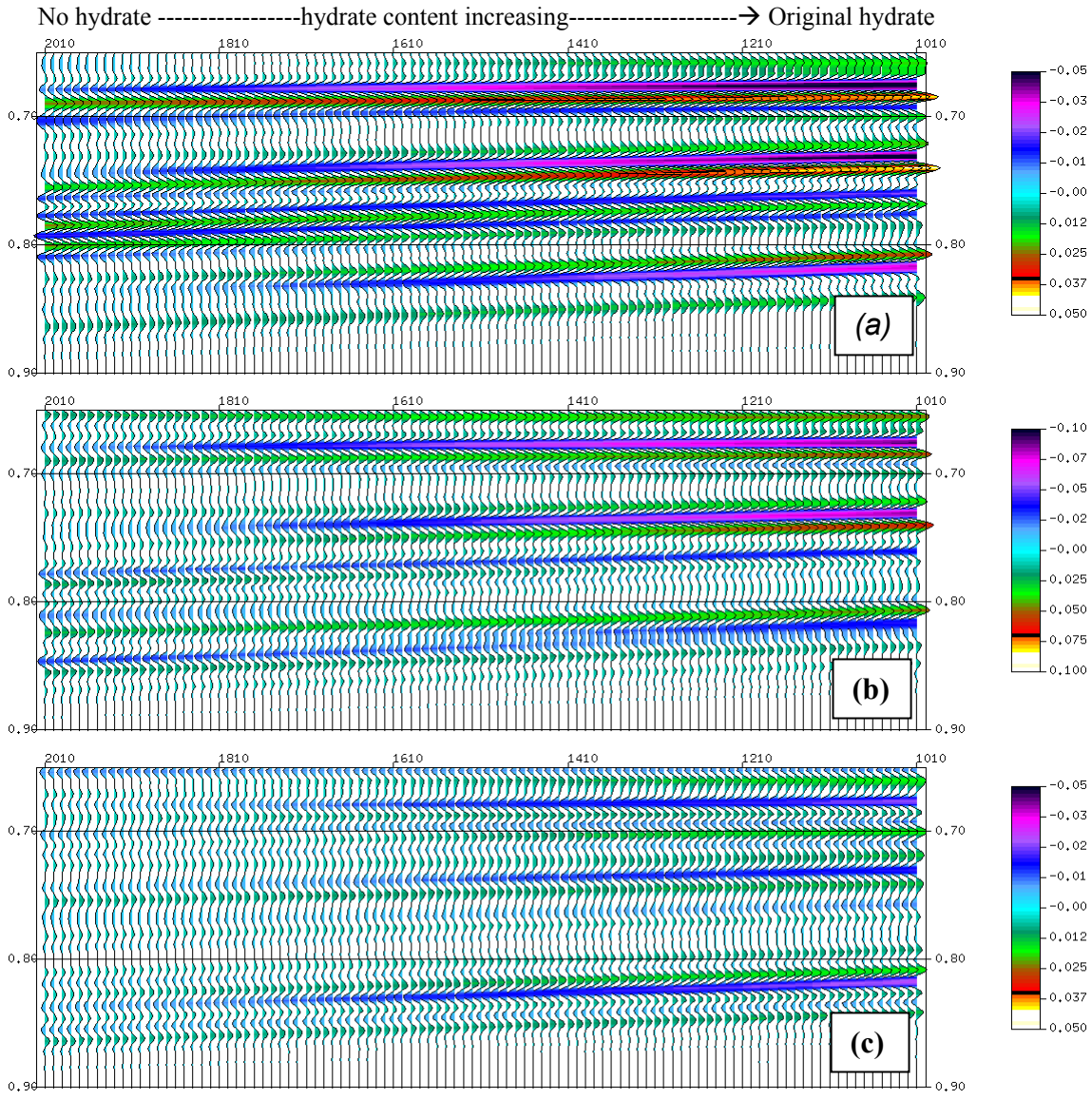

Fig. 9: P and S velocity reflectivity from 2D model and fluid factor sections: (a) P velocity reflectivity; (b) S velocity reflectivity; (c) fluid factor.

AVO responses and AVO-derived attributes – fluid factor help to map the hydrate distribution. To estimate the hydrate concentration more accurately, it is necessary to obtain P or S velocity mapping. 2L-38 shows that high concentration of hydrate causes a dramatic increase in P wave velocity, which may affect the traveltimes of seismic wave. So stacking velocity and its conversion to interval velocity help to estimate the hydrate concentration. Ecker et al. used such information to estimate hydrate amount (Ecker et al., 2000). Here, the velocity picking and conversion to interval velocity are performed using the 2D model dataset in Figure 9 to evaluate the sensitivity of velocity from seismic data to the hydrate amount.

Fig. 10 shows the velocity analysis of CDP gathers at original 2L-38 location and at zero hydrate concentration location. The interval velocity converted from picked stack velocity is compared with well logs. Hydrate concentration is shown up as large average blocks.

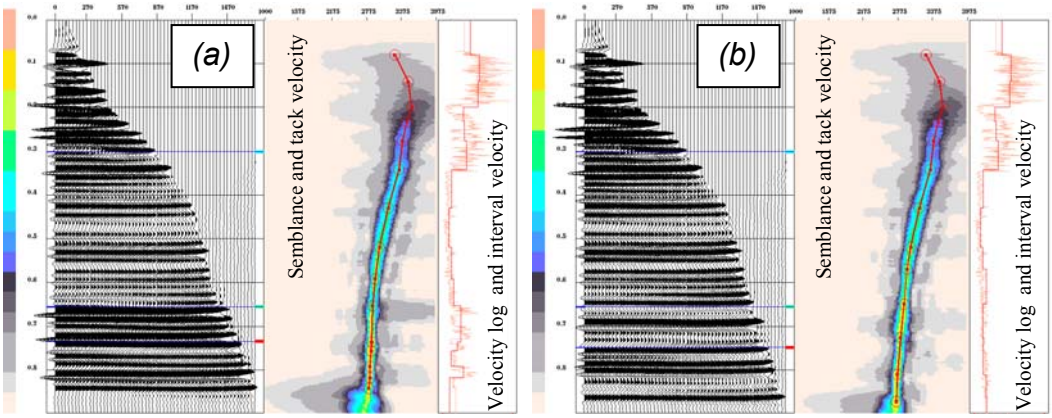

Fig. 10: Gathers, semblance, velocity picking, conversion to interval velocity and well logs (a) at original hydrate concentration CDP location and (b) zero hydrate concentration CDP location.

Fig. 11 shows a 2D section of interval velocity mapping converted from RMS velocity picked on semblances. The lateral variation due to hydrate concentration can be clearly seen with the resolution limited by seismic data frequency band.

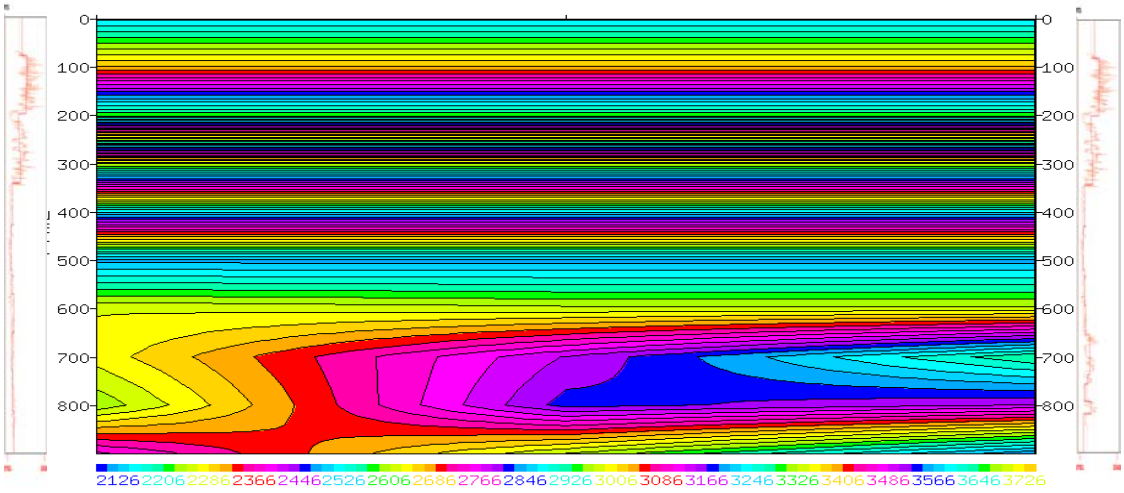

Fig. 11. 2D interval velocity mapping from picked RMS velocities at different hydrate concentration CDP locations.

So far, either AVO anomaly or interval velocity converted from stacking velocity indicates the existence of high hydrate concentration. In Mackenzie Delta, most of the drilling occurred in Tertiary and late Cretaceous sequences. The velocity increases gradually with burial depth. In the depth of hydrate accumulation zones, the rock is unconsolidated clastic. It is not usual that a large-scale tight

rock body with high velocity inserts in the soft rocks. Therefore, the abnormally high velocity might be interpreted as high hydrate concentration. However, often large error, exists in the interval velocity converted from stack velocity, due to the insensitivity of stacking velocity and the complex structures above the velocity anomaly. Therefore, amplitude and AVO anomaly should be incorporated into the interpretation to exclude the ambiguities.

Conclusions and discussions

P and S velocity from 2L-38 show the sensitivity to hydrate concentration. AVO response and fluid factor show the strongly anomaly caused by high hydrate concentration. To uniquely decide the existing of large scale hydrate distribution, the pre-stack seismic data is required to perform AVO analysis, incorporated with velocity from seismic data, such as the interval velocity converted from stack velocity.

References

Collett, T., Lewis, R., Dallimore, S., Lee, M., Mroz, T., and Uchida, T., 1999, Mallik 2L-38 downhole well log displays – Detailed evaluation of gas hydrate reservoir properties, in Dalimore, S., Uchida, T., and Collett, T. Eds., Scientific results from JAPEX/JNOC/GSC Mallik 2L-38 gas hydrate research well, Mackenzie Delta, NWT, Canada: Geol. Surv. Can. Bull., 544, 295-311.

Ecker, C., Dvorkin, J., and Nur, A., 1998, Sediments with gas hydrates: internal structure from seismic AVO: Geophysics, 1659 – 1669.

2000, Estimating the amount of gas hydrate and free gas from marine seismic data: Geophysics, 565 - 573.

Guerin, G., and Goldberg, D., 2002, Sonic waveform attenuation in gas hydrate-bearing sediments from the Mallik 2L-38 research well, Mackenzie Delta, Canada: Journal of Geophysical Research, Vol. 107, No. B5.

Lee, M., 2002, Biot-Gassmann theory for velocities of gas hydrate-bearing sediments: Geophysics, 1711-1719.

Lee, M., and Collett, T., 2001, Elastic properties of gas hydrate-bearing sediments: Geophysics, 763 – 771.

Marvko, G., Mukerji, T., and Dvorkin, J., 1998, The rock physics handbook: Cambridge University Press.

Northern Oil and Gas Directorate, Petroleum exploration in northern Canada – A guide to oil and gas exploration and potential: 1995, Indian and Northern Affairs Canada.